# Design and Finite Element Analysis of a Radial-Flux Salient-Pole Eddy Current Brake

Ali SINMAZ[1], Mehmet Onur GULBAHCE[2], and Derya Ahmet KOCABAS[2]

[1]Dept. of Electrical Power Engineering RWTH Aachen, Aachen, Germany
ali.sinmaz@rwth-aachen.de
[2]Dept. of Electrical Engineering, Istanbul Technical University, Istanbul, Turkey
ogulbahce@itu.edu.tr, kocabasde@itu.edu.tr

## Abstract

**This paper presents a novel design containing design constraints and analysis of a radial-flux salient pole Eddy current brake whereby performance characteristics and design principles are given. In order to obtain an optimal brake design, different design models based on different parameters are all analyzed by using finite element method (FEM). Eventually, an optimized radial-flux salient pole eddy current brake design having more effective cooling capability than that of the conventional one is purposed. Results for the analysis are presented together with advantages and disadvantages.**

***Keywords—Eddy currents, eddy current brakes, electromagnetic brake systems, finite element analysis***

## 1. Introduction

When a conductive material is exposed to a time-varying magnetic flux, eddy currents are induced inside the material due to the change in the magnetic flux according to Faraday's law. Eddy currents complete their path along the material as a loop and they create a magnetic field opposing the applied one [1]. Furthermore, induced eddy currents deplete the mechanical energy electrically at the rate of the product of square of the effective value of eddy current (I2) and the resistance of the conductive material (R) [2,3]. Besides depending on the polarities of the two magnetic fields, they weaken each other and a braking force is generated. The eddy current brakes are widely used for slowing down a moving object such as a train, roller coaster or any vehicle and also for load tests of electrical machines. Unlike the conventional brake systems, the eddy current brakes are frictionless and less damage crops up in the materials used in the design of the brake [4]. Also system response of the brake is more sustainable and less maintenance is needed [5, 6].

Differential equations are needed to associate the input and output data of an eddy current brake system. The complexity of the system makes it difficult to solve this complex mathematical formulation. Two known methods can be used to obtain the time response of the whole system. First method is using numerical methods such as finite-element analysis (FEA), and the second one is to solve the system equation analytically. In addition to these, the parametric analysis can be used for first design stage [7, 8 and 9].

In conventional Eddy current brakes, the conductive disc is placed in front of the magnets or electromagnets [10, 11]. This design forces the flux to complete its path axially causing the brake to be called axial-flux design. Axial design have several design constraints including the conductivity, thickness and magnetic properties of the disc, length of air-gap, number of poles and excitation current. In practice, this design has disadvantages in cooling, since the total power dissipation inside the disc can cause a tremendous temperature rise bringing about changes in the electrical, magnetic and geometric properties of the disc. These changes can affect the braking performance of the system.

In main study, a novel design for an eddy current brake forcing the flux to complete its path radially is investigated. The rotor has a salient-pole design similar to the traditional synchronous machine. Unlike the axial-flux design, the conductive disc is placed around the rotor poles in a ring shape. First of all, design parameters are obtained for the chosen rated value by analytical calculations on magnetic equivalent circuit (MEC) model. Then the design is optimized by means of FEA. Effects of design constraints like electrical, magnetic and geometric properties of the conductive material around the poles, excitation current and air-gap length are all analyzed. Contribution of using a back iron frame (carcass) around the conductive ring is also investigated. In the novel design, windings placed around salient poles are needed to produce the flux while the flux travels among a cylindrically shaped conductive material. This structure serves a better cooling performance by the contribution of the increased cooling area than that of the conventional eddy current brakes at the same rated values. Having an outer conductive disc provides the availability of additional plate-fins placement around material to improve cooling.

In this paper, as a part of the main study, the FEA results for two optimized designs are given. The first design does not have a ferromagnetic cover around the conductive disc and the second design does. The results are obtained for different angular speed values to access the change of braking torque and total power dissipation versus speed for each brake designs.

## 2. General Theory of Eddy Current Brake

Eddy current brakes are composed of a stationary magnetic flux source like permanent magnet or electromagnet and a conductive disc connected to a rotating mechanical energy source. Depending on rotation, the conductive material exposed to a time varying magnetic flux density which can be expressed by Lenz's law where E is electric field intensity and B is magnetic flux density [10].

$$\nabla \times \vec{E} = -\frac{\partial \vec{B}}{\partial t} \tag{1}$$

Occurrence of electric field causes current, because of Ohm's law where J is current density and these currents are eddy currents which complete their path along the material as a loop.

$$\vec{J} = \sigma \cdot \vec{E} \tag{2}$$

The action between eddy currents and magnetic flux density creates a braking force (F) and induced braking torque can be expressed as below, where r is the radius of the disc;

$$\vec{F} = \vec{J} \times \vec{B} \tag{3}$$

$$\vec{T} = \vec{F} \cdot r \tag{4}$$

## 3. Finite Element Equations

Eddy current brakes include stationary poles creating the magnetic field which are excited by excitation current or permanent magnets and moving conducting disc. In practise eddy current brakes have non-conducting and conducting regions to be modelled by using magnetic scalar potential $\vartheta$ and magnetic vector potential A where $H_T$ is total magnetic field intensity [10]. In non-conducting regions (5) is used.

$$H_T = -\nabla.\vartheta \tag{5}$$

This total magnetic field intensity has two components including $\phi$ as reduced magnetic scalar potential and $H_S$ as the magnetic field intensity of source.

$$H_T = -\nabla.\phi + H_S \tag{6}$$

The relation between $H_S$ and $J_S$, source current density is as shown below.

$$\nabla \times H_S = J_S \tag{7}$$

The Laplacian type equation is below where $\mu$ is the permeability;

$$\nabla.\mu.\nabla.\vartheta = 0 \tag{8}$$

In eddy current or conducting regions B, magnetic flux density and E, electric field intensity can be expressed as below where V is scalar electric potential, $\varpi$ is speed [6].

$$B = \nabla \times A \tag{9}$$

$$E = -\frac{\partial A}{\partial t} - \nabla.V + \varpi \times \nabla \times A \tag{10}$$

In order to obtain an equation where V is omitted, equation 2, 10, and Ampère's law can be used;

$$\nabla \times \frac{1}{\mu} \times \nabla \times A = \sigma\left(-\frac{\partial A}{\partial t} - \varpi \times \nabla \times A + \nabla.V\right) \tag{11}$$

Eq. 12 is attained by obtaining the divergence of (11).

$$\nabla.\sigma\left(-\frac{\partial A}{\partial t} - \varpi \times \nabla \times A + \nabla.V\right) = 0 \tag{12}$$

Scalar electric potential can be expressed in terms of A and $\varpi$ as in (13).

$$V = A.\varpi \tag{13}$$

By substituting (13) into (11),

$$\nabla \times \frac{1}{\mu} \times \nabla \times A = \sigma\left(-\frac{\partial A}{\partial t} - (\varpi.\nabla)A - (A.\nabla)\varpi - A \times (\nabla \times \varpi)\right) \tag{14}$$

is obtained.

## 4. Design of Radial-Flux Salient-Pole Eddy Current Brake

This paper presents a part of the main study. In the main study, a radial-flux salient pole ECB is designed and optimized for the targeted name plate data. The optimized design is then analyzed for two different operating conditions. First, the design is analyzed without a ferromagnetic cover around the conductive ring called as back-iron. Afterwards, same design including the cylindrical ferromagnetic cover in order to provide a smoother path for magnetic flux is analyzed.

As mentioned in the Introduction, an unconventional design is obtained in order to improve the cooling capabilities of ECB. Rotating disc and stationary excitation windings exchange their roles with each other in the novel design. The excitation windings to be fed by DC current are placed around salient poles to produce the actual magnetic flux and the shaft placed in the center of the poles helps the poles to rotate. The conductive disc is transformed into a conductive ring surrounding the rotating poles so as to help the flux to complete its path.

In order to provide a better comparison of different designs by authors, major design constraints such as air-gap flux density, pole surface area, number of turns per coil, excitation current and the thickness of the conductive disc obtained in the previous studies [4,7] are implemented in the novel design.

It is obvious that, depending on the nature of operational principle of the ECB, same design constraints will affect the performance of the brake. However, the description of some design parameters is replaced with an equivalent one depending on the nature of axial and radial design geometry.

The initial point for the new design is the air-gap flux density value used in the previous studies [4-7]. In order to calculate Ampere-turn values and the mean radius magnetic flux density in air gap pole pitch of the conductive disc is used. Length of the path of magnetic flux inside the aluminum disc shown in Fig. 1. is also needed to be calculated. Other design parameters are inner, outer and mean radius of the conductive ring $r_i$, $r_o$ and $r_m$, respectively, air gap length g, number of pole pairs p, pole pitch $\tau_p$ and pole shoe width $d_p$ as it can be seen in Fig. 1. Used equations are given in (14-17) where $B_g$ is magnetic flux density, $H_T$ is the total magnetic field density, $l_{Al}$ is the path length inside the ring , N is number of turns, i is excitation current and $\mu_0$ is the magnetic permeability of air that is assumed equal to permeability of conductive disc. Magnetic permeability of poles and back-iron is accepted infinite in design

calculations for simplicity, but B-H curve of steel 1010 is used during FEA.

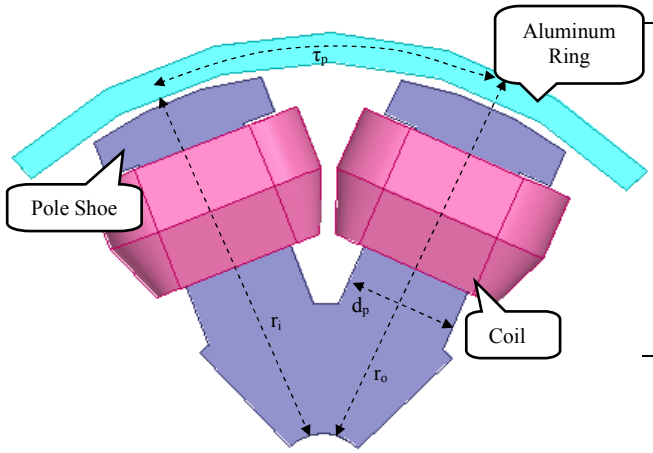


**Fig.1.** Top view of the radial – flux salient pole *ECB*

$$r_m = \frac{r_i + r_o}{2} \tag{14}$$

$$l_{Al} = \frac{\tau_p}{360^\circ} \cdot 2\pi \cdot r_m \tag{15}$$

$$2 \cdot N \cdot i = 2\left(H_g \cdot l_{air}\right) + H_{Al} \cdot l_{Al} \tag{16}$$

$$H_g = H_{Al} = \frac{B_g}{\mu_0} \tag{17}$$

Steel-1010 is used as the magnetic material for the poles and the back-iron in the brake, aluminum 7075 is used as conductive ring, copper is used for wiring. Optimized design parameters are given in Table I.

Same calculations are done for the design with a back iron. In this case, since the magnetic reluctance of a back iron is almost zero comparing to aluminum and air-gap, total length of the magnetic equivalent circuit is equal to sum of length of air gap and thickness of conductive ring.

Second design to be analyzed is obtained by addition of back-iron having an minimum thickness to prevent saturation as seen in Fig. 2. Increase in the thickness does not have any negative significant effect on the magnetic flux, but affects cooling performance. Magnetic flux density increases since the leaked flux intends to use back-iron to complete its path resulting in an increase in the flux density of the aluminum ring. The total flux intends to be increased by the existence of back-iron, although the length of the magnetic path is increased slightly depending on the thickness of back-iron.

Both designs are analyzed in the same way. Skin depth meshed algorithm is used in the conductive ring in order to obtain accurate results. Depending on the symmetry, only ¼ of the real geometry is used. Simulation results are given and compared in the next section.

**Table 1.** Design Parameters of ECB

| Parameter | Quantity | Value |
|---|---|---|
| $r_o$, $r_i$ | Inner and outer radius of ring | 139.5, 130.5 *mm* |
| $r_m$ | Mean radius of ring | 135 *mm* |
| $g$ | Air-gap thickness | 2 *mm* |
| $p$ | Number of pole pairs | 4 |
| $\tau_p$ | Pole Pitch | 45˚ |
| $d_p$ | Pole body width | 35 *mm* |
| $r_2$, $r_1$ | Inner and outer radius | 149.5, 130.5 *mm* |
| $w_2$, $w_1$ | Back-iron and ring thickness | 10, 9 *mm* |
| $\sigma_{Al}$ | Conductivity of ring | 26770000 *S/m* |
| $\mu_r$ | Permeability of ring | 1 |
| $N$ | Number of turns per pole | 300 |
| $i$ | Excitation current | 10 *A* |

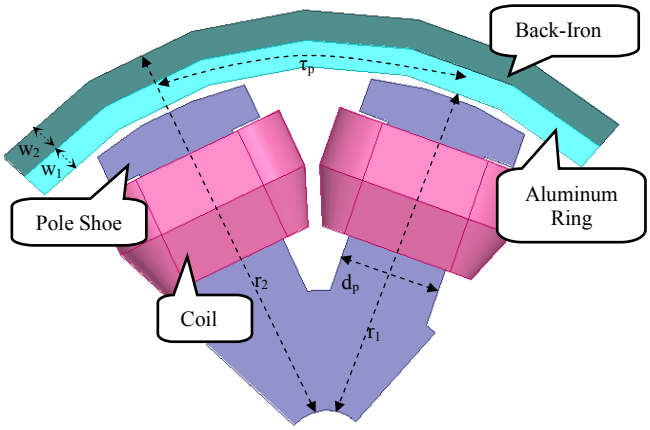


**Fig.2.** Top view of the radial – flux salient pole ECB with back-iron

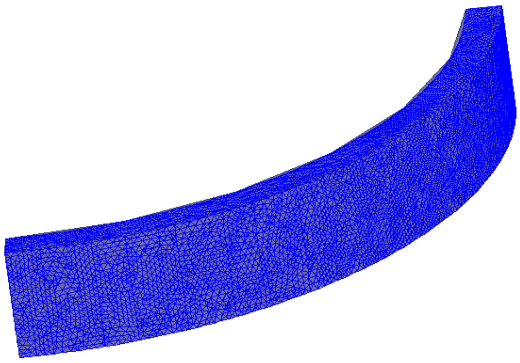

**Fig.3.** Mesh structure of the aluminum ring

## 5. Simulation Results

The two designs are analyzed for different speed values and the results are combined to obtain integrated torque-speed and total power dissipation-speed characteristics. To visualize the benefits of the novel designs, only the results of one simulation for each are given for the speed value of 3000 $min^{-1}$. The results are given in Fig. 4-8. Fig. 4 illustrates the distribution of magnetic flux density on rotor.

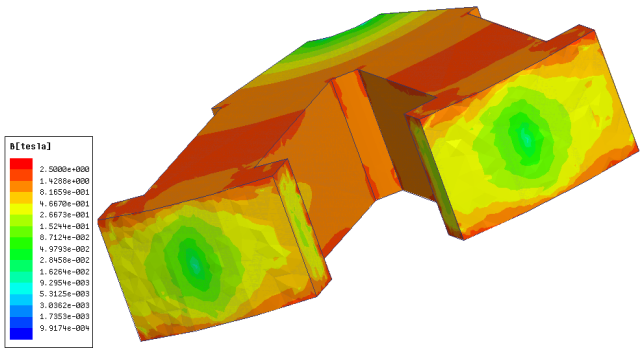


**Fig.4.** Distribution of magnetic flux density on the surface of pole shoes

Fig. 5 and 6 demonstrate the distribution of magnetic flux density on the surface of the conductive ring without and with back iron, respectively. The design with a back iron provides a more saturated magnetic flux density than that of the one without back-iron as explained in the previous section.

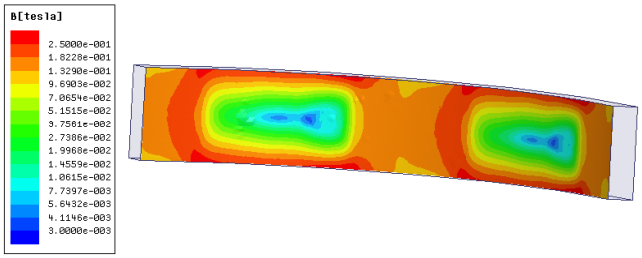


**Fig. 5.** Distribution of magnetic flux density on the surface of the conductive ring without a back-iron

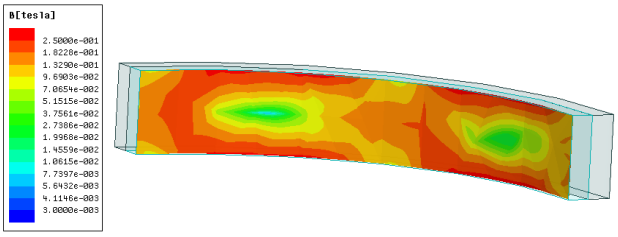


**Fig. 6.** Distribution of magnetic flux density on the surface of the conductive ring with a back-iron

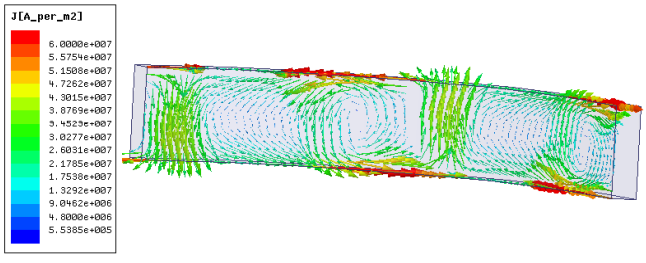


**Fig.7.** Eddy current vector distribution on the surface of the conductive ring without a back-iron

Eddy current vector distributions for each design are plotted in Fig. 7 and 8. Back-iron design is given in Fig. 8.

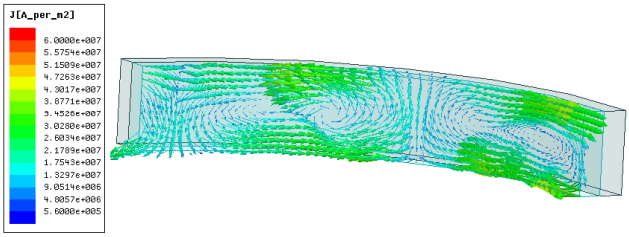


**Fig. 8.** Eddy current vector distribution on the surface of the conductive ring with a back-iron

Eddy current vectors are denser at the edges of the material as expected. Nonetheless, these loop formed currents have distinct densities with a lower leakage in the design with a back-iron and eddy Current vectors are distributed more evenly. Since the return paths of eddy currents are lengthened better braking torque for the same speed is induced.

Fig. 9 and 10 includes the comparison of characteristics for both designs. Curves in both figures are obtained by combining the results of simulations for different speed values between 0 and 7500 min-1.

Fig. 9 shows the comparison of torque vs speed and Fig. 10 includes the comparison of total power dissipation vs speed curves.

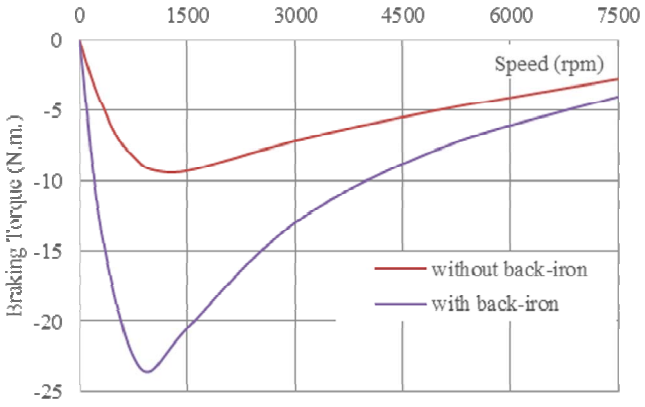


**Fig. 9.** Braking Torque-Speed Characteristic of ECB

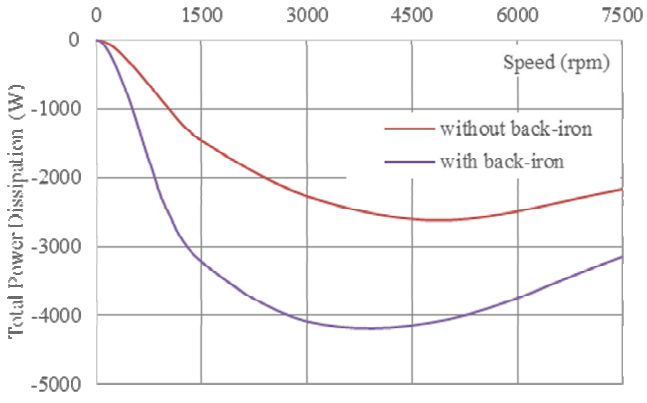


**Fig. 10.** Total Power Dissipation-Speed Characteristic of ECB

## 6. Conclusion

A novel design for a radial flux, wound excited, salient-pole ECB is presented. Design constraints and operational quantities are all given. A back-iron cover ring is proposed to improve the flux density distribution among the conductive ring. Two different types of new design are analyzed by using FEA for different angular speed values. In order to visualize the benefits of the designs, only results for one simulation for 3000 $min^{-1}$ is displayed. Integrated torque-speed and total power dissipation-speed curves are obtained and compared.

Since this paper presents a part of a main study, it is possible to make comparison with the previously obtained data [4, 7]. It can be seen that radial flux ECB provides better pull-out braking torque for the same air-gap flux density, pole surface area, excitation current, total number of turns, air-gap length and conductive disc thickness.

For the comparison of the designs with and without back-iron, it can be mentioned that the design having back-iron ring around the conductive ring performs better than the other one for all low, medium and high speed values. The ratio of the maximum braking torque values of both designs is approximately 2.5 at pull-out point. Mechanical behavior properties are improved in the one having back-iron. Use of back-iron helps for a more even Eddy Current distribution resulting in a better braking torque production.

Basic disadvantage for the novel ECB design is the difficulties for the control of braking torque around the pull-out point. Nevertheless, better braking torque is always obtainable when compared to axial flux ECB.

Total power dissipation is increased in the design having back-iron. But this disadvantage can be tolerated by increasing the cooling area without causing an increase in inertia and a change in flux density in the conductive ring. Additional cooling ribs can also be added.

Investigating braking torque and total power dissipation characteristics highlights the design with a back iron theoretically.

## 7. References


[1] E. J. Davies, “General Theory of Eddy Current Couplings and Brakes”, *Proceedings of the Institution of Electrical Engineers*, vol. 113, no.5, pp. 825-837, May 1966

[2] H. Sodano, J. Bae, “Eddy current damping in structures”, *The Shock and Vibration Digest*, vol. 36, no.6, pp. 469-478, November 2004.

[3] A. F. Mergen, D. A. Kocabas, “Elektrik Makinalarında Sargılar (Windings in Electrical Machines)”, 1st ed. (in Turkish), Istanbul: Birsen Yayınevi, 2007

[4] M. O. Gulbahce, “Orta Guclu Bir Girdap Akimi Freni Tasarimi ve Sonlu Elemanlar Yöntemi ile Analizi (Design and Finite Element Analysis of a Medium PowerEddy Current Brake)”, Msc. Thesis, Istanbul Technical University, Graduate School of Science Engineering and Technology, 2012

[5] D. Schieber, “Braking Torque on Rotating Sheet in Stationary Magnetic Field, *Proceedings of the Institution of Electrical Engineers*, vol. 121, no. 2, pp. 117–122.,1974

[6] D. Rodger, H. C. Lai, P. K. Vong, “Finite Element Model of Eddy Current Brake”. *The Fourth International Conference on Computation in Electromagnetics (CEM 2002) (Ref. No. 2002/063)*

[7] M. O. Gulbahce, D. A Kocabas0, I. Habir, “Finite Element Analysis of a Small Power Eddy Current Brake”, *Mechatronica, 2012, IEEE Conference*, 5-7 December, 2012

[8] M. O. Gulbahce, D. A Kocabas, A. K Atalay, “A Study to Determine the Act of Excitation Current on Braking Torque for a Low Power Eddy Current Brake”, *IEMDC-13, IEEE Conference*, 12-15 May 2013 Chicago-Illinois.

[9] M. O. Gulbahce, D. A Kocabas, D. A, Atalay A. K., “Determination of the Effect of Conductive Disk Thickness on Braking Torque for a Low Power Eddy Current Brake”, *POWERENG-13, IEEE Conference*, 13 – 17 May 2013, Istanbul, Turkey.

[10] S. E.Gay, M. Ehsani, “Analysis and experimental testing of permanenet magnet eddy current brake”, *Vehicle Power and Propulsion, 2005, IEEE Conference*, 7-9 September, 2005.

[11] R.Yazdanpanah, M. Mirsalim, “Axial-Flux wound excitation eddy current brakes: Analytical study and parametric modelling”, *IEEE Trans. Magn.*, vol. 50, no. 6, pp. 1-10, Jun. 2014

[12] M. V. K. Chari, “Finite Element Solution of the Eddy-Current Problem in magnetic Structures”, *IEEE Transactions on Power Apparatus and Systems*, vol. PAS-93, no. 1, pp. 62-72

[13] M.O, Gulbahce, D.A Kocabas, F Nayman, "Investigation of the effect of pole shape on braking torque for a low power eddy current brake by finite elements method," *8th International Conference on Electrical and Electronics Engineering (ELECO), 2013*, vol., no., pp.263-267, 28-30 Nov. 2013

[14] M.O. Gulbahce, H. Nak, D.A. Kocabas, "Design of a mechanical load simulator having an excitation current controlled eddy current brake," *3rd International Conference on Electric Power and Energy Conversion Systems (EPECS), 2013*, vol., no., pp.1-5, 2-4 Oct. 2013